A Novel Method for the Estimation of the Elastic Modulus of Ultra-High Performance Concrete using Vibration Data

Duong Huong Nguyen
Hanoi University of Civil Engineering, Vietnam
duongnh2@huce.edu.vn

Samir Khatir
Center for Engineering Application & Technology Solutions, Ho Chi Minh City Open University, Ho Chi Minh City, Vietnam
khatir_samir@hotmail.fr

Quoc Bao Nguyen
Hanoi University of Civil Engineering, Vietnam
baonq@huce.edu.vn (corresponding author)

Received: 17 May 2024 | Revised: 31 May 2024 | Accepted: 5 June 2024

 DOI: https://doi.org/10.48084/etasr.7859

ABSTRACT

The elastic modulus of concrete is one of the most important parameters in the analysis and design of concrete structures. However, determining the elastic modulus in civil structures using core-drilled samples is time-consuming and labor-intensive. Additionally, the elastic modulus of Ultra-High Performance Concrete (UHPC) varies significantly depending on its composition. This paper proposes an improved, non-destructive application to identify the elastic modulus of UHPC materials in in-service structures. The elastic modulus is estimated through calibration between a numerical model and experimental UHPC plate vibration test results, using frequency and mode shapes. This calibration involves solving an inverse problem using optimization techniques such as Particle Swarm Optimization (PSO), Genetic Algorithm (GA), Cuckoo Search, and the YUKI algorithm. Updating the plate characteristics is made possible by the development of numerous iterations, where each iteration updates the elastic modulus, thickness, and width values in the term to find the best solution. The highest accuracies compared to experimental data natural frequency values were found in models updated by GA, PSO, YUKI, and Cuckoo algorithms, with errors of 10.77%, 6.58%, 6.87%, and 6.87%, respectively. An experimental sample was tested to determine the elastic modulus of the UHPC, and the proposed application showed a 0.55% error compared to the experimental value. Thus, the estimated elastic modulus value is highly accurate.

Keywords-accelerometers; elastic modulus; experimental analysis; model updating; UHPC

I. INTRODUCTION

Concrete is widely used in various construction sectors. Various types of concrete have been developed, including Plain Cement Concrete (PCC), Reinforced Cement Concrete (RCC), Self-Compacting Concrete (SCC), High-Performance Concrete (HPC), Ultra-High Performance Concrete (UHPC), and Reactive Powder Concrete (RPC). Among these, UHPC stands out due to its ability to reduce structural size, enhance strength, facilitate unique architectural designs, ensure high-quality construction, allow rapid assembly, and lower construction costs despite its high initial expense [1]. UHPC's advantages, including low maintenance cost, long life cycle, and economic efficiency, make it widely used in civil and bridge structures [1-4]. Civil structures can suffer damage due to weather, environmental conditions, and external forces, necessitating regular Structural Health Monitoring (SHM). SHM based on vibration data analysis is a non-destructive testing method that provides accurate results [5, 6]. This approach has been used since the '70s, initially for offshore projects and later expanding to other industries, including construction and aerospace. Various studies have proposed methods for evaluating the SHM of bridges [7-9]. The elastic modulus is crucial for analyzing concrete structures and identifying damage. However, it varies over time, making it essential to know its value at the time of the survey. Typically, compressive strength

tests determine the elastic modulus of UHPC [10], but these can be inaccurate due to uncertain operational parameters. Core-drilled sample tests, while accurate, are challenging, expensive, and time-consuming. Non-destructive methods have been developed for this purpose. For instance, authors in [11] used wave tomography techniques, combining ultrasonic pulse velocity and shear wave velocity tests for more accurate estimates. Author in [12] combined ultrasonic pulse velocity and echo methods, whereas others have used X-ray computed tomography [13] and machine learning algorithms [14] to predict the elastic modulus.

Vibration-based methods, using transducers like Linear Variable Differential Transformers (LVDTs), accelerometers, and strain gauges, are suitable for in-service structures. The measurement data, typically recorded in the time domain, can be transformed into the frequency domain using Fourier transforms [15-18]. Analyzing vibration response data helps identify dynamic parameters such as natural frequency and mode shape, which are affected by the structure's physical characteristics like density, elastic modulus, and boundary conditions. Thus, the elastic modulus can be precisely specified by updating models based on structural vibration response. Authors in [19] successfully updated a numerical model of a UHPC bridge in Malaysia, achieving a maximum difference of 4.16% between the numerical and the experimental models. Authors in [20] tested the Nam O Railway bridge in Vietnam, updating the model based on measurement results with a maximum natural frequency deviation of 8.57% in the first 10 modes. In this study, a UHPC plate with dimensions of 3,500 mm × 500 mm × 40 mm with simply supported boundary conditions is considered.

II. THE FINITE ELEMENT MODEL

A Finite Element (FE) model was created in Matlab using the Partial Differential Equation Toolbox [21]. The details of the FE model are as follows:

- The measured plate dimensions are 3,500 mm × 489.6 mm × 43.2 mm along the x, y, and z axes, respectively.
- The UHPC plate is modeled using three-dimensional (solid) elements.
- Supports for the UHPC plate are positioned 250 mm from the plate's ends. One is a fixed support, and the other is a movable support. These supports are in contact with the UHPC plate along its width in the experimental model. In the numerical model, the supports are represented with spring nodes.
- The numerical model incorporates the following material properties: elastic modulus, volumetric mass density, and Poisson's ratio of the UHPC material. The elastic modulus is typically calculated through compressive strength or specimen testing. Various formulas establish the connection between elastic modulus and compressive strength, often derived from experiments or the literature. The elastic modulus of UHPC, which ranges from 40 GPa to 55 GPa or higher, is strongly influenced by the material's composition [1-2, 22]. Initially, an elastic modulus of 45 GPa is used in the FE model. This value will be updated based on experimental results using inverse analysis. The volumetric mass density ranges from 2,350 kg/m³ to 2,550 kg/m³, depending primarily on the fiber composition [1-2, 22]. The mass density used in the FE model is 2,410.7 kg/m³. Poisson's ratio is assumed to be 0.2.

Figure 1 shows the first four vertical bending natural frequencies and mode shapes. The natural frequencies are 9.366 Hz, 36.994 Hz, 81.279 Hz, and 138.401 Hz for Mode 1, Mode 2, Mode 3, and Mode 4, respectively. In the next section, a comparative study between numerical and experimental results is presented. Model updating will be analyzed to improve the numerical model for more effective results.

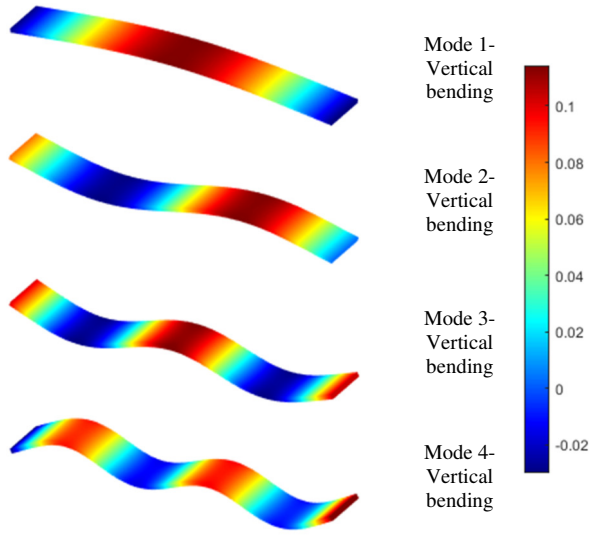

Fig. 1. First four bending frequencies and mode shapes of a UHPC plate.

III. EXPERIMENTAL MODEL

A. Experimental Setup

Material: The plate is constructed with UHPC. The typical basic grade of UHPC includes fine sand, quartz powder, silica fume, cement, fiber reinforcement, superplasticizer, and water. Various grades have been developed based on local material availability [22]. This specific grade of UHPC has been previously used in several civil structures [23].

Boundary conditions: The two ends of the UHPC plate, positioned 250 mm from the end, rest on two steel supports. One support is movable and shaped like a steel cylinder with a diameter of 50 mm and a length of 600 mm. The other support is fixed and shaped like a steel prism with a length of 600 mm and a cross-section of an equilateral triangle with 60 mm sides. Figure 2 illustrates these supports.

Plate dimensions: The formwork dimensions for the UHPC plate were 3,500 mm length, 500 mm width, and 40 mm thickness. Figure 3 shows the UHPC plate after removing the formwork at the LAS-XD 125 Laboratory of Hanoi University of Civil Engineering. Manufacturing the formwork precisely was challenging, leading to slight deviations in width from the original design. After formwork removal, the plate dimensions

were re-measured, yielding an average width of 489.6 mm and an average thickness of 43.2 mm.

Location of equipment and accelerometers: Fifteen accelerometers were used to measure the natural frequencies and mode shapes of this plate. These sensors were placed on the top side of the UHPC plate in five evenly spaced rows horizontally and eleven rows longitudinally. The sensitivity of these accelerometers ranges from 10.13 to 10.5 mV/m.s². The arrangement of the accelerometers in the laboratory is shown in Figures 4 and 5. This setup was divided into five setups, each containing 15 accelerometers, as detailed in Table I. Each setup included five fixed measuring points/accelerometers (reference nodes) to link the measured data across all setups. National Instruments (NI) equipment and a laptop were used to record the accelerometer data. A hammer was used as the excitation force, struck at various points between the two supports on the top side of the UHPC plate.

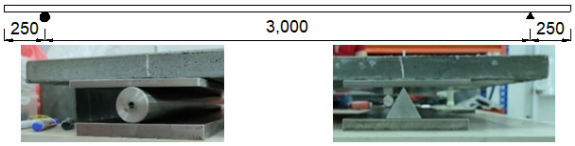

Fig. 2. Support placement.

Fig. 3. UHPC plate after removing the formwork.

TABLE I. MEASUREMENT SETUP

Setup	Number of accelerometers														
	1	**2**	**3**	**4**	**5**	**6**	**7**	**8**	**9**	**10**	**11**	**12**	**13**	**14**	**15**
1	1	2	3	**4**	5	6	7	8	9	10	11	**41**	**28**	**14**	**49**
2	12	13	15	**4**	16	17	18	19	20	21	22	**41**	**28**	**14**	**49**
3	23	24	25	**4**	26	27	29	30	31	32	33	**41**	**28**	**14**	**49**
4	34	35	36	**4**	37	38	39	40	42	43	44	**41**	**28**	**14**	**49**
5	45	46	47	**4**	48	50	51	52	53	54	55	**41**	**28**	**14**	**49**

Note: the bold digits in this table (4, 14, 28, 41 and 49) represent the reference nodes

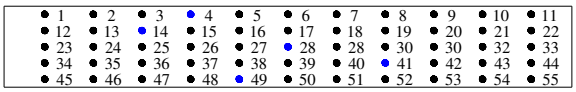

Fig. 4. Accelerometerss layout.

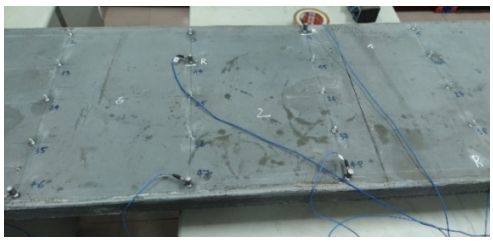

Fig. 5. Arrangement of accelerometers in the plate.

B. *Experimental Results*

Each setup underwent measurements, with data collected over 300 s at a sampling rate of 2,560 Hz. The Stochastic Subspace Identification algorithm was employed to analyze the accelerometer data, enabling the determination of the certainty and stability of the natural frequencies. Stabilization diagrams were generated for 1% frequency, 5% damping, and 1% mode shape accuracy, as depicted in Figure 6. Utilizing these parameters, the natural frequencies for the first four bending modes were determined as 9.49 Hz, 41.46 Hz, 86.83 Hz, and 141.41 Hz for modes 1, 2, 3, and 4, respectively. The experimentally extracted mode shapes are illustrated in Figure 7.

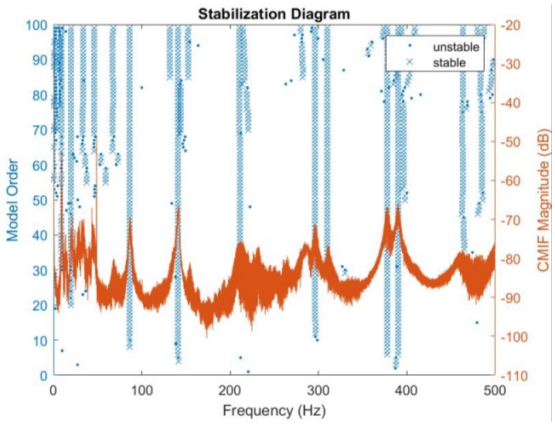

Fig. 6. The stabilization diagram.

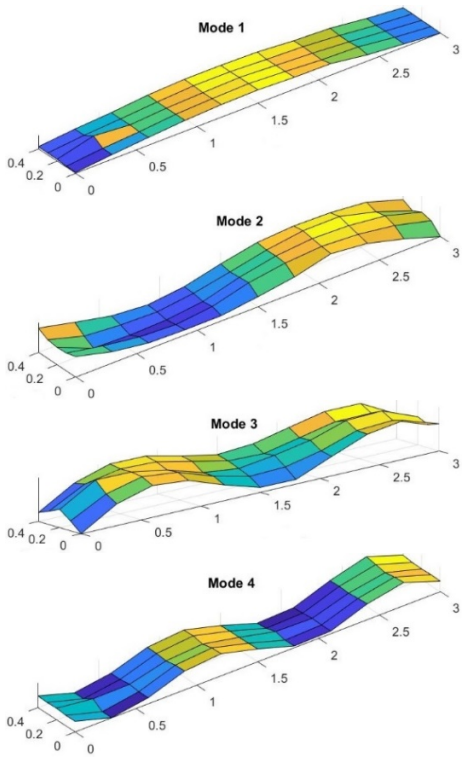

Fig. 7. The first four bending modes identified from the experiment.

IV. MODEL UPDATING

1) Theoretical Background

To upđate the above numerical model and determine the necessary parameters, the following optimization algorithms were considered:

2) Genetic Algorithm

Genetic Algorithm (GA) is one of the most popular optimization algorithms. This algorithm leverages the natural selection principle (selection, crossover, and mutation) [24]. An initial population is initially created, consisting of several individuals with unique traits. The less resilient individuals will eventually be eliminated. Only those with better traits to endure are left (natural selection). The crossover process creates new individuals that inherit the traits of two parents. The primary determinant of whether a population can evolve is a mutation, a minor random change in a few individuals' chromosomes. After that, the procedure is repeated until the termination condition is met.

3) Particle Swarm Optimization (PSO) Algorithm

PSO was developed in 1985 [25]. A school of fish or flock of birds can benefit from the collective experience, enabling more effective movement. In PSO, particle positions are initially randomized within a predetermined constrained range, and their objective function values is calculated. Each particle's best position and the group's best position are identified. Then, particle velocities and positions are updated based on these best positions. This process repeats until a termination condition is met, such as achieving the objective function value or reaching a set number of iterations.

4) Cuckoo Algorithm

The Cuckoo algorithm was developed in 2009 [26]. This algorithm is built from the parasitic habits of cuckoos. Because they never build nests, these birds lay their eggs in the nests of other host birds. When treating each egg in the nest as a solution, the cuckoo egg is seen as the new and good solution. If the host bird finds strange eggs that are not his own, he will either throw these eggs away or simply abandon his nest and build another one. The best nests with high egg quality will be carried over to the next generation.

5) YUKI Algorithm

The YUKI algorithm, introduced in 2021 [27], is a new metaheuristic approach that dynamically reduces the search space by creating a smaller region around the current best result. It uses the distance between locations to adjust the search area size. The algorithm calculates local boundaries and performs two types of searches: one focusing on the center of the search area and the other outside it. As iterations progress, the focus shifts from exploration to exploitation. Randomly generated values determine the exploration population size, and new solutions are generated based on these values. The best solutions are updated at each iteration.

B. Model Updating UHPC Plate Parameters

The natural frequencies of the UHPC plate were determined through testing post-fabrication, as detailed in Section III. The finite element method was employed to simulate this plate in Section II, but certain data in the numerical model, such as the elastic modulus or UHPC plate dimensions, may harbor uncertainty and require adjustment based on experimental findings. To identify the elastic modulus of an in-service structure, a detective method is often employed. This involves extracting drill specimens for subsequent laboratory testing, albeit limited to local areas. In this study, the PSO, the GA, the Cuckoo Search, and the YUKI algorithm are utilized to update the elastic modulus of UHPC. The natural frequencies are leveraged to formulate the following objective function:

$$\text{Objective function} = \sum_{i=1}^{n} \left[100 \times \frac{f_{Exp} - f_{FE}}{f_{Exp}} \right]^2 \quad (1)$$

where f_{FE}, f_{Exp} represent the natural frequencies of the numerical model and the experimental model, respectively, and n denotes the number of considered modes.

GA, YUKI, Cuckoo, and PSO algorithms were utilized to determine the elastic modulus of UHPC based on (1), considering the first four bending modes, with the best results of the 1,000 iterations shown in Table II. In this instance, the GA converged faster than the others with 235 iterations, whereas YUKI converged the slowest with 943 iterations. The objective functions of the YUKI, Cuckoo, and PSO algorithms have approximately the same value (≈ 62.24119), which is smaller than the value obtained by the GA algorithm (≈ 62.61434). More specifically, the objective function reaches the smallest value when using the PSO algorithm, followed by Cuckoo, YUKI, and GA. When considering the mean, the worst, and the standard deviation, it is found that the YUKI algorithm gives less convergent results than the others. Table III summarizes the results of the natural frequencies of the first four vertical bending modes in the following situations: (1) before model updating, (2) after updating by GA, (3) after updating by YUKI, (4) after updating by Cuckoo, (5) after updating by PSO, and (6) experimental measurement. In general, the results before and after updating are close to the experimental results. The natural frequencies provided by YUKI, Cuckoo, or PSO are more aligned with the experimental frequencies than GA, likely because PSO finds and returns the best global positions of particles whereas ignoring the local best. The YUKI, Cuckoo, and PSO algorithms yield similar results. However, Cuckoo converges faster than PSO and YUKI. The thickness and width of the UHPC plate, along with the elastic modulus, need to be updated as described in Section III. Updating these parameters simultaneously often yields numerous and sometimes irrational results. To address this, we propose a sequential model updating approach for each parameter:

- First, using fixed thickness h and width b values (initially taking the measured values from Section III), update the elastic modulus E.
- Next, adjust thickness h while keeping the updated elastic modulus E, and width b fixed.
- Then, with thickness h and elastic modulus E fixed, update the width b.
- Repeat until the convergence condition is met.

TABLE II. NATURAL FREQUENCIES BASED ON NUMERICAL AND EXPERIMENTAL MODELS

No	Mode	Frequency (Hz)					
		Before updating	**Updating with GA**	**Updating with YUKI**	**Updating with Cuckoo**	**Updating with PSO**	**Experimental data**
1	1st vertical bending	9.366	9.798	9.768	9.768	9.768	9.49
2	2nd vertical bending	36.994	38.732	38.614	38.613	38.613	41.46
3	3rd vertical bending	81.279	87.912	87.644	87.644	87.644	86.83
4	4th vertical bending	138.401	145.216	144.773	144.773	144.773	141.41
No	**Mode**	**Differences to experimental data (%)**					
		Before updating	**Updating with GA**	**Updating with YUKI**	**Updating with Cuckoo**	**Updating with PSO**	**Experimental data**
1	1st vertical bending	1.31%	3.24%	2.93%	2.93%	2.93%	-
2	2nd vertical bending	10.77%	6.58%	6.87%	6.87%	6.87%	-
3	3rd vertical bending	6.39%	1.25%	0.94%	0.94%	0.94%	-
4	4th vertical bending	2.13%	2.69%	2.38%	2.38%	2.38%	-
Sum			163.1	62.6143415	62.2411972	62.2411969	62.2411967

TABLE III. BEST RESULTS OF THE OBJECTIVE FUNCTIONS

Algorithm	**GA**	**YUKI**	**Cuckoo**	**PSO**
Best	62.6143415	62.2411972	62.2411969	62.2411967
Mean	67.1400479	238.3899123	72.1779759	70.9736488
Worst	868.7997062	866.1567975	652.7777915	868.7997062
Standard deviation	52.1127604	223.4116759	64.7415731	55.0473033
Number of iterations	235	943	676	789
Elastic modulus (Pa)	49,214,230,628	48,914,876,673	48,914,636,624	48,914,695,403

This iterative process revises the values of E, h, and b to account for measurement errors from the tools and the personnel. It is important to note that the optimization algorithm is applied to update each parameter sequentially. Table IV lists the outcomes. The convergence condition is met at the 12th iteration, where the values of the elastic modulus, thickness, width, and the objective function remain constant.

TABLE IV. RESULTS OF E, H AND B AFTER MODEL UPDATING

No	***E* (Pa)**	***h* (m)**	***b* (m)**	$f_{objective}$	**Convergence condition**
0	45,000,000,000	0.0432	0.4896		
1	48,914,613,043	0.0432	0.4948	61.3072	
2	49,126,989,555	0.0432	0.4956	61.0699	
3	49,146,161,186	0.0432	0.4961	61.0552	
4	49,161,160,249	0.0432	0.4961	61.0527	
5	49,146,989,249	0.0432	0.4961	61.0499	
6	49,126,255,227	0.0432	0.4962	61.0448	
7	49,113,453,538	0.0432	0.4958	61.0509	
8	49,096,405,496	0.0433	0.4962	61.0409	
9	49,089,995,470	0.0433	0.4961	61.0408	
10	49,080,193,179	0.0433	0.4962	61.0379	
11	49,065,869,616	0.0433	0.4962	61.0361	
12	**49,062,377,696**	**0.0433**	**0.4962**	**61.0360**	**OK**
13	49,062,377,696	0.0433	0.4962	61.0360	OK
14	49,062,377,696	0.0433	0.4962	61.0360	OK
15	49,062,377,696	0.0433	0.4962	61.0360	OK

V. EXPERIMENTAL ELASTIC MODULUS

The elastic modulus test was conducted on the UHPC plate to verify the accuracy of the proposed method, following ASTM C469 - Standard Test Method for Static Modulus of Elasticity and Poisson's Ratio of Concrete in Compression. The test specimen was a cylinder, 200 mm in height and 100 mm in diameter. Figure 8 shows the load test performed at the Hanoi University of Civil Engineering's Laboratory LAS-XD 125, with a load rate of 1.0 MPa/s applied to the UHPC specimen [22]. This test involved three cycles of loading and unloading. Using the measured applied force, specimen dimensions, and strain values (obtained from three strain gauges: two axial and one perpendicular), the stress-strain curve was plotted. Figure 9 presents the experimental setup and instrumentation. The stress-strain curve in Figure 9 was used to calculate the elastic modulus. The test specimens were weighed to determine the volumetric mass density of the UHPC material, which was found to be 2410.7 kg/m³.

Fig. 8. Determining the elastic modulus of UHPC material (compressing test and laboratory instruments).

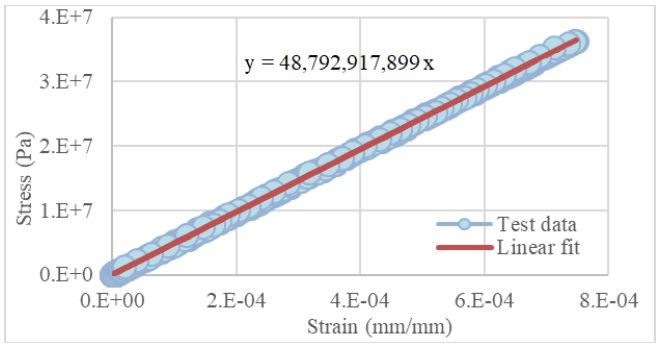

Fig. 9. Stress–strain curve.

The experimental mean value of the elastic modulus, determined using a linear trend line with an R-squared value of 0.9998, was 48,792,917,899 Pa. The updated elastic modulus (49,062,377,696 Pa, see Section IV) deviates by only 0.55% from the experimental data, demonstrating the accuracy of the proposed application.

VI. CONCLUSIONS AND RECOMMENDATIONS

This study demonstrates a method for identifying the elastic modulus of UHPC materials in in-service structures. By updating the numerical model based on the results of UHPC plate vibration tests, specifically natural frequencies and mode shapes, the elastic modulus can be estimated. The process consists of four main steps: (1) building a numerical model, (2) fabricating an experimental model, (3) performing experiments to determine the vibrational characteristics, and (4) updating the numerical model based on these characteristics.

The experimental model and dynamic test results depend on the composition of the UHPC material. The first four bending modes are identified by installing 15 accelerometers in the longitudinal direction and five in the transverse direction. Numerical model updating is performed using optimization algorithms: Genetic Algorithm (GA), Particle Swarm Optimization (PSO), Cuckoo algorithm, and YUKI algorithm. In addition to determining the elastic modulus, the plate thickness and width are adjusted to account for measurement errors. The elastic modulus, thickness, and width values were updated after each iteration. The results show that the objective function value of PSO is smaller than that of GA, indicating that the PSO algorithm performs better in this context. The results from the YUKI and Cuckoo algorithms are almost the same with those from PSO. The updated elastic modulus value shows a 0.55% deviation from the experimental value, demonstrating the accuracy of the proposed method. The highest inaccuracies in natural frequencies, compared to experimental data, are found in the second mode with values of 10.77% (GA), 6.58% (YUKI), and 6.87% (Cuckoo and PSO). The proposed method employs vibration data and optimization algorithms to determine the global elastic modulus and certain geometric characteristics of in-service structures, particularly those utilizing UHPC materials, providing a non-destructive approach with potential applications in structural health monitoring.

The properties of UHPC material are highly dependent on fiber distribution and type [28], making it essential to control the mixing and pouring process to ensure uniform fiber reinforcement. Future research directions include determining the elastic modulus of a real UHPC bridge using vibration data, employing the estimated elastic modulus for structural health monitoring, and considering material characteristics based on the construction age.

ACKNOWLEDGMENT

Duong Huong Nguyen was funded by the Postdoctoral Scholarship Programme of Vingroup Innovation Foundation (VINIF), code VINIF.2022.STS.54.

REFERENCES

[1] H. G. Russell, B. A. Graybeal, and Inc. Henry G. Russell, "Ultra-high performance concrete : a state-of-the-art report for the bridge community," Office of Infrastructure Research & Development, Federal Highway Administration, McLean, VA, USA, FHWA-HRT-13-060, Jun. 2013.

[2] E. Fehling, M. Schmidt, J. Walraven, T. Leutbecher, and S. Fröhlich, *Ultra-High Performance Concrete UHPC: Fundamentals, Design, Examples*. New York, NY, USA: John Wiley & Sons, 2015.

[3] D. Bierwagen and A. Abu-Hawash, "Ultra High Performance Concrete Highway Bridge," in *Mid-Continent Transportation Research Symposium*, Ames, IA, USA, Aug. 2005, pp. 1–14.

[4] C. Ozyildirim, "Evaluation of Ultra-High-Performance Fiber-Reinforced Concrete," Virginia Center for Transportation Innovation Research, Charlottesville, VA, USA, FHWA/VCTIR 12-R1, Aug. 2011.

[5] C. R. Farrar and S. W. Doebling, "Damage Detection and Evaluation II," in *Modal Analysis and Testing*, J. M. M. Silva and N. M. M. Maia, Eds. Dordrecht, Netherlands: Springer, 1999, pp. 345–378.

[6] M. S. Mohammed and K. Ki-Seong, "Chirplet Transform in Ultrasonic Non-Destructive Testing and Structural Health Monitoring: A Review," *Engineering, Technology & Applied Science Research*, vol. 9, no. 1, pp. 3778–3781, Feb. 2019, https://doi.org/10.48084/etasr.2470.

[7] N. N. Long, N. H. Quyet, N. X. Tung, B. T. Thanh, and T. N. Hoa, "Damage Identification of Suspension Footbridge Structures using New Hunting-based Algorithms," *Engineering, Technology & Applied Science Research*, vol. 13, no. 4, pp. 11085–11090, Aug. 2023, https://doi.org/10.48084/etasr.5983.

[8] A. E. Aktan, F. N. Catbas, K. A. Grimmelsman, and C. J. Tsikos, "Issues in Infrastructure Health Monitoring for Management," *Journal of Engineering Mechanics*, vol. 126, no. 7, pp. 711–724, Jul. 2000, https://doi.org/10.1061/(ASCE)0733-9399(2000)126:7(711).

[9] L. Fryba and M. Pirner, "Load tests and modal analysis of bridges," *Engineering Structures*, vol. 23, no. 1, pp. 102–109, Jan. 2001, https://doi.org/10.1016/S0141-0296(00)00026-2.

[10] R. W. Sun and G. C. Fanourakis, "An assessment of factors affecting the elastic modulus of concrete," *Structural Concrete*, vol. 23, no. 1, pp. 593–603, 2022, https://doi.org/10.1002/suco.202000553.

[11] M. A. Hadianfard, H. Marzouk, and C. Shafieyanb, "Strength and elastic moduli of a concrete bridge using advanced nondestructive techniques," *Scientia Iranica*, vol. 24, no. 3, pp. 942–952, Jun. 2017, https://doi.org/10.24200/sci.2017.4078.

[12] I. Ivanchev, "Experimental determination of dynamic modulus of elasticity of concrete with ultrasonic pulse velocity method and ultrasonic pulse echo method," *IOP Conference Series: Materials Science and Engineering*, vol. 1252, no. 1, Jun. 2022, Art. no. 012018, https://doi.org/10.1088/1757-899X/1252/1/012018.

[13] A. Alshahrani, S. Kulasegaram, and A. Kundu, "Elastic modulus of self-compacting fibre reinforced concrete: Experimental approach and multi-scale simulation," *Case Studies in Construction Materials*, vol. 18, Jul. 2023, Art. no. e01723, https://doi.org/10.1016/j.cscm.2022.e01723.

[14] Q. Zhang and M. Afzal, "Retracted: Prediction of the elastic modulus of recycled aggregate concrete applying hybrid artificial intelligence and machine learning algorithms," *Structural Concrete*, vol. 23, no. 4, pp. 2477–2495, 2022, https://doi.org/10.1002/suco.202100250.

[15] D. H. Nguyen, T. T. Bui, G. De Roeck, and M. Abdel Wahab, "Damage detection in Ca-Non Bridge using transmissibility and artificial neural networks," *Structural Engineering and Mechanics*, vol. 71, no. 2, pp. 175–183, Jan. 2019, https://doi.org/10.12989/sem.2019.71.2.175.

[16] D. H. Nguyen, Q. B. Nguyen, T. Bui-Tien, G. De Roeck, and M. Abdel Wahab, "Damage detection in girder bridges using modal curvatures gapped smoothing method and Convolutional Neural Network: Application to Bo Nghi bridge," *Theoretical and Applied Fracture Mechanics*, vol. 109, Oct. 2020, Art. no. 102728, https://doi.org/10.1016/j.tafmec.2020.102728.

[17] N. M. M. Maia, J. M. M. Silva, E. A. M. Almas, and R. P. C. Sampaio, "Damage detection in structures: from mode shape to frequency response function methods," *Mechanical Systems and Signal Processing*,

vol. 17, no. 3, pp. 489–498, May 2003, https://doi.org/10.1006/mssp.2002.1506.

[18] Y. J. Yan, L. Cheng, Z. Y. Wu, and L. H. Yam, "Development in vibration-based structural damage detection technique," *Mechanical Systems and Signal Processing*, vol. 21, no. 5, pp. 2198–2211, Jul. 2007, https://doi.org/10.1016/j.ymssp.2006.10.002.

[19] S. S. Saidin *et al.*, "Operational modal analysis and finite element model updating of ultra-high-performance concrete bridge based on ambient vibration test," *Case Studies in Construction Materials*, vol. 16, Jun. 2022, Art. no. e01117, https://doi.org/10.1016/j.cscm.2022.e01117.

[20] H. Tran-Ngoc, S. Khatir, G. De Roeck, T. Bui-Tien, L. Nguyen-Ngoc, and M. Abdel Wahab, "Model Updating for Nam O Bridge Using Particle Swarm Optimization Algorithm and Genetic Algorithm," *Sensors*, vol. 18, no. 12, Dec. 2018, Art. no. 4131, https://doi.org/10.3390/s18124131.

[21] "MathWorks - Makers of MATLAB and Simulink." https://www.mathworks.com/.

[22] A. Alsalman, C. N. Dang, G. S. Prinz, and W. M. Hale, "Evaluation of modulus of elasticity of ultra-high performance concrete," *Construction and Building Materials*, vol. 153, pp. 918–928, Oct. 2017, https://doi.org/10.1016/j.conbuildmat.2017.07.158.

[23] H. D. Pham, T. Khuc, T. V. Nguyen, H. V. Cu, D. B. Le, and T. P. Trinh, "Investigation of flexural behavior of a prestressed girder for bridges using nonproprietary UHPC," *Advances in concrete construction*, vol. 10, no. 1, pp. 71–79, 2020, https://doi.org/10.12989/acc.2020.10.1.071.

[24] M. Mitchell, *An Introduction to Genetic Algorithms*. Cambridge, MA, USA: MIT Press, 1998.

[25] J. Kennedy and R. Eberhart, "Particle swarm optimization," in *International Conference on Neural Networks*, Perth, WA, Australia, Dec. 1995, vol. 4, pp. 1942–1948, https://doi.org/10.1109/ICNN.1995.488968.

[26] X.-S. Yang and S. Deb, "Cuckoo Search via Levy flights," in *World Congress on Nature & Biologically Inspired Computing*, Coimbatore, India, Dec. 2009, pp. 210–214, https://doi.org/10.1109/NABIC.2009.5393690.

[27] B. Benaissa, N. A. Hocine, S. Khatir, M. K. Riahi, and S. Mirjalili, "YUKI Algorithm and POD-RBF for Elastostatic and dynamic crack identification," *Journal of Computational Science*, vol. 55, Oct. 2021, Art. no. 101451, https://doi.org/10.1016/j.jocs.2021.101451.

[28] J. Li and Z. Deng, "Tensile behavior of ultra-high performance concrete reinforced with different hybrid fibers," *Structural Concrete*, vol. 24, no. 1, pp. 1415–1435, 2023, https://doi.org/10.1002/suco.202200353.